# Average and local structure of α-CuI by configurational averaging



2007 J. Phys.: Condens. Matter 19 466208

(http://iopscience.iop.org/0953-8984/19/46/466208)

IOP PUBLISHING JOURNAL OF PHYSICS: CONDENSED MATTER

J. Phys.: Condens. Matter **19** (2007) 466208 (18pp) doi:10.1088/0953-8984/19/46/466208

# Average and local structure of $\alpha$-CuI by configurational averaging

**Chris E Mohn**[1] **and Svein Stølen**

Department of Chemistry and Centre for Materials Science and Nanotechnology, University of Oslo, PO Box 1033 Blindern, N-0315 Oslo, Norway

E-mail: chrism@kjemi.uio.no

Received 8 August 2007, in final form 27 September 2007
Published 23 October 2007
Online at stacks.iop.org/JPhysCM/19/466208

**Abstract**

Configurational Boltzmann averaging together with density functional theory are used to study in detail the average and local structure of the superionic $\alpha$-CuI. We find that the coppers are spread out with peaks in the atom-density at the tetrahedral sites of the fcc sublattice of iodines. We calculate Cu–Cu, Cu–I and I–I pair radial distribution functions, the distribution of coordination numbers and the distribution of Cu–I–Cu, I–Cu–I and Cu–Cu–Cu bond-angles. The partial pair distribution functions are in good agreement with experimental neutron diffraction—reverse Monte Carlo, extended x-ray absorption fine structure and *ab initio* molecular dynamics results. In particular, our results confirm the presence of a prominent peak at around 2.7 Å in the Cu–Cu pair distribution function as well as a broader, less intense peak at roughly 4.3 Å. We find highly flexible bonds and a range of coordination numbers for both iodines and coppers. This structural flexibility is of key importance in order to understand the exceptional conductivity of coppers in $\alpha$-CuI; the iodines can easily respond to changes in the local environment as the coppers diffuse, and a myriad of different diffusion-pathways is expected due to the large variation in the local motifs.

(Some figures in this article are in colour only in the electronic version)

## 1. Introduction

The structure of superionic CuI ($\alpha$-CuI) has been extensively investigated for more than 50 years. In an early study, the coppers were assumed to be randomly distributed over all tetrahedrally coordinated positions within a rigid fcc array of iodines, with an appreciable fraction (approximately 25%) located at the octahedral positions (see figure 1) [1]. This model has been supported by extended x-ray absorption fine structure (EXAFS) results [2] and also by

[1] Author to whom any correspondence should be addressed.

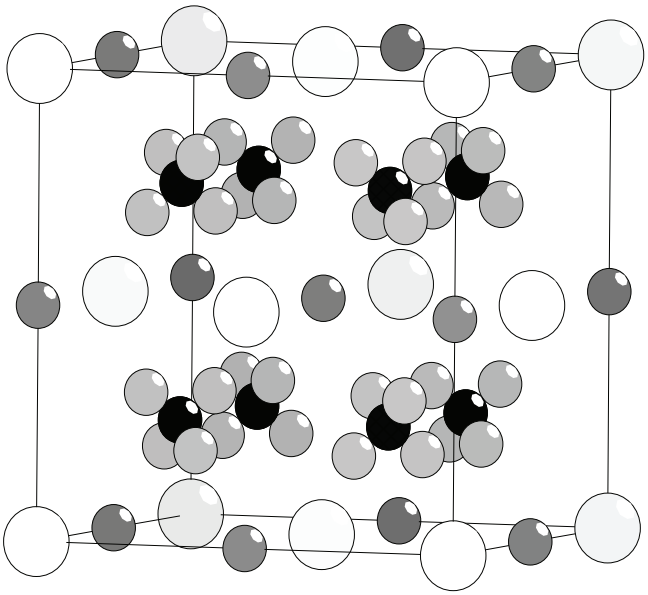

**Figure 1.** A collection of possible crystallographic models for the average structure of $\alpha$-CuI. The iodines are shown as big white spheres. The dark grey, black and light grey are the coppers at octahedral 4b, tetrahedral 8c and the 'interstitial' 32f site (which are the sites on a straight line connecting the tetrahedral 8c and the nearest octahedral 4b position (i.e. at the positions $(x, x, x)$ etc)).

molecular dynamics (MD) simulations using pair potentials [3], but several neutron diffraction (ND) studies [4–7] and MD simulations [8] (using very similar potentials to that of [3]) indicate that the octahedral positions are not occupied [4–7]. The apparent discrepancy between the MD simulation in [3] and that of [8] was traced to different interpretations of the mean ionic density within the simulations and was explained because the coppers exhibit large anharmonic vibrations along the $\langle 111 \rangle$ direction and occasionally venture into the octahedral holes [3, 7]. This 'anharmonic behaviour' can reasonable well be modelled by a random distribution of the coppers at the 32f site (at e.g. $(x, x, x)$ etc with $x = 0.30$) of the space group $Fm\bar{3}m$ [4, 5] (see figure 1) but a better fit to the observed x-ray diffraction data was found by distributing 80% of the coppers randomly over the 8c site and the remaining 20% randomly over the 32f site [9].

Although the average structure is reasonably well described in terms of crystallographic concepts, the detailed description of atom correlation between the coppers is debated. This is shown in figure 2 where we have collected some previously reported Cu–Cu pair radial distribution functions (PDFs). The thin full line is the Cu–Cu PDF derived from neutron diffraction data by reverse Monte Carlo (ND-RMC) modelling [6] and the thick full line is due to an EXAFS study [10]. The ND-RMC and EXAFS are in qualitative agreement but show notable differences in that the first peak in the ND-RMC curve is wider than that of EXAFS. Whereas the RMC analysis of the ND data indicates that the Cu–Cu distances can be as short as 1.9 Å, the EXAFS study suggests that the shortest distance between the Cu atoms is 2.4 Å [10]. Results from MD simulations [8, 11] are also plotted in figure 2 as dotted lines. As can be seen from the figure, the MD simulations using pair potentials (thin dotted line) are not in qualitative agreement with the ND-RMC and EXAFS results at short Cu–Cu distances (the first peak in the Cu–Cu PDF is absent) [3, 8]. By contrast, the quantum mechanical MD study reported in [11]

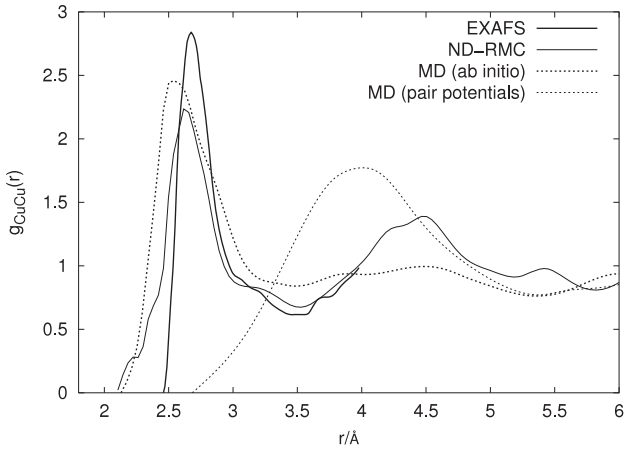


**Figure 2.** Different Cu–Cu pair distribution functions reported in the literature for $\alpha$-CuI. The EXAFS [10] (at $T = 693$ K), ND-RMC [6] (at $T = 713$ K), *ab initio* molecular dynamics (at $T = 700$ K) [11] and MD simulations using pair potentials [8] (at $T = 763$ K) are shown as thick and thin full lines and thick and thin dotted lines respectively.

is able to describe short range copper–copper correlation but the second peak at around 4.3 Å appears too 'smeared out' in comparison with experiment.

In spite of the lack of agreement in the literature, the Cu–Cu PDFs shown in figure 2 all emphasize that atom correlations are non-negligible and that the PDFs are very different from that expected by distributing the coppers over the average 8c and 32f sites determined by x-ray powder diffraction [9]. Whereas the random distribution model predicts an intense peak close to 3 Å, corresponding to the simultaneous occupation of the nearest tetrahedral (8c) site of the average structure, the first peak in the Cu–Cu PDF in all MD-DFT, EXAFS and ND-RMC PDFs are at significantly shorter distance and closer to an 8c–32f separation. Also, the peaks in the PDFs are smooth and broad; similar to that of liquid CuI [12] indicating that the atoms are *not* located at distinct sites. Indeed, the RMC analysis of ND data [6] and results from x-ray powder diffraction [9] show that the coppers are spread out in the tetrahedral holes. Consequently, while $\alpha$-CuI is long range ordered due to the 'rigid' I sublattice the *instantaneous* structure of $\alpha$-CuI is expected to show a large variation *locally*. These local motifs cannot be deduced from models of the average structure. Analysing the local structure and atom correlations is crucial in order to understand the exceptional transport properties of $\alpha$-CuI.

In this work we investigate the local structure and atom correlation of $\alpha$-CuI using configurational Boltzmann averaging (CA) in conjunction with density functional theory. We have in previous papers presented the configurational averaging technique, see for instance [13–15], which involves mapping the individual basins on the potential energy surface (PES) of a periodic simulation cell *independently* followed by Boltzmann averaging. We assume that interbasin 'jumps' and intrabasin movements on the potential energy surface occur at different timescales so that we can break the system partition function into pure configurational and vibrational contributions. That is, events associated with bond formation and bond breaking are assumed to be rare compared to a typical vibrational frequency. Results from calculations on superionic conductors indicate that this assumption is reasonable also within the superionic regime. Calculations on, for example, superionic $Li_3N$ indicate that the average residence time (intrabasin movements) is about one order of magnitude larger than the average 'flight time' (interbasin jumps) [16]. *Pure* configurational properties can thus be

evaluated in the static limit by mapping the minima on the PES and vibrational contributions (thermal excitations of each of the local minima) can subsequently be extracted.

An important advantage with the CA method over conventional methods (e.g. molecular dynamics) is that the CA method is not hampered by the presence of potential energy barriers and thus is particularly well designed for the study of long time dynamics such as configurational disorder.

## 2. Theory

In this work we map the configurational space by means of optimizing a set of initial arrangements constructed by distributing the ions on an underlying grid. We assume that the grid is designed such that the structural optimizations provide a one-to-one map of all initial arrangements to *all* basin minima [17]. The optimizations are carried out within the generalized gradient approximation (GGA), using the Perdew–Wang 91 functional [18] for the exchange–correlation contribution to the total energy as implemented in the Vienna *ab initio* simulation program [19, 20]. Test calculations indicate that a constant plane-wave energy cutoff of 400 eV and a uniform $2 \times 2 \times 2$ Monkhorst–Pack grid were sufficient for the present purpose. Ignoring vibrations, configurational properties are subsequently calculated as Boltzmann averages over the distinct local minima on the system potential energy surface. The ensemble average of the quantity $Y$ evaluated in the *static limit* is thus given as

$$\langle Y \rangle = \frac{\sum_{l=1}^{K} Y^l \exp\left(\frac{-E^l}{k_B T}\right)}{\sum_{l=1}^{K} \exp\left(\frac{-E^l}{k_B T}\right)}, \tag{2.1}$$

where $K$ is the total number of minima (associated with the distinct basins on the system PES). $E^l$ is the minimized potential energy of arrangement $l$ and $k_B$ is Boltzmann's constant.

In this work we evaluate the partial PDFs using an equation analogous to (2.1). The radial distribution of atoms of type $j$ around a given atom of type $i$ is given as

$$\langle g_{ij}(r) \rangle = \frac{\sum_{l=1}^{K} g_{ij}^l(r) \exp\left(\frac{-E^l}{k_B T}\right)}{\sum_{l=1}^{K} \exp\left(\frac{-E^l}{k_B T}\right)}, \tag{2.2}$$

where

$$g_{ij}^l(r) = \frac{n_{ij}^l(r)}{4\pi r^2 \Delta r \rho_i^l}. \tag{2.3}$$

Here $n_{ij}^l(r)$ is the number of $j$ atoms in a thin sphere with thickness $\Delta r$ centred at a given atom of type $i$ ($\Delta r = 0.2$ Å in the calculations), and $\rho_i^l$ is the mean particle density of $i$ of configuration $k$. The coordination numbers (CN), that is the average number of atoms of type $j$ around a given atom of type $i$, can be extracted using

$$\langle N_{ij} \rangle = \frac{\sum_{l=1}^{K} N_{ij}^l \exp\left(\frac{-E^l}{k_B T}\right)}{\sum_{l=1}^{K} \exp\left(\frac{-E^l}{k_B T}\right)}, \tag{2.4}$$

where

$$N_{ij}^l = \int_{r=0}^{r=r_{\max}} n_{ij}^l(r) r \, dr. \tag{2.5}$$

Here $r_{\max}$ is the maximum cutoff radius (see below).

For the average (unnormalized) bond-angle distribution (BAD) function, $f_{ijk}(\theta)$, we use the following expression

$$\langle f_{ijk}(\theta)\rangle = \frac{\sum_{l=1}^{K} n_{ijk}^{l}(\theta)\exp\left(\frac{-E^{l}}{k_{\mathrm{B}}T}\right)}{\sum_{l=1}^{K}\exp\left(\frac{-E^{l}}{k_{\mathrm{B}}T}\right)}, \tag{2.6}$$

where $n_{ijk}^{l}(\theta)$ is the number of angles within a small interval $\Delta\theta$ from a given central atom of type $i$ to a pair of atoms $j$ and $k$ located within some distance $r_{\max}$ from the central atom. In the calculations we used $\Delta\theta = 5^{\circ}$ and the choice of cutoff distance of the first coordination shell ($r_{\max}$) was based on an inspection of the first peak in the Cu–Cu and Cu–I partial PDFs. $r_{\max}$ was 3.1 Å in the calculations of the bond-angle distributions and the coordination numbers.

### *2.1. Strategies for mapping the individual basins on the PES*

Calculations of ensemble averages using equation (2.1) involve the enumeration of all $K$ minima which is, for all but the most trivial examples, computationally unfeasible. Strategies for the *a priori* selection of a small but representative number ($K'$) of all possible arrangements is thus required. We have previously presented a series of complimentary strategies for the efficient selection of a small fraction of all arrangements for the accurate calculation of configurational properties of disordered materials. These strategies involve a random selection, the use of symmetry, radial distribution functions and genetic algorithms [14, 21, 22].

In the random selection strategy, initial arrangements are chosen at random and the convergence of the ensemble average with number of optimized configurations is analysed. A few randomly chosen arrangements have been sufficient for the calculation of thermodynamic and structural properties in oxide [21], mineral [13] and alloy [23] solid solutions at high $T$, when a large fraction of all minima is populated. However, in order to analyse the convergence of the ensemble averages with number of configurations we must first construct an appropriate grid where we distribute the atoms for the structural optimizations. We thus initially investigate the energetic preference of the different possible sites using a small conventional eight-atom simulation cell.

### *2.2. Preliminary test calculations*

The initial configurations of the eight-atom cell are constructed by distributing the ions at random over a grid containing the tetrahedral 8c, the octahedral 4b and an 'interstitial' 32f (e.g. at $(x, x, x)$ etc with $x = 0.375$), see figure 1. This grid is fairly uniform and is designed such that it does not bias any particular site of the average structure when the coppers are distributed at random over the grid. A large fraction of 50 randomly and symmetrically distinct arrangements were selected. In addition, we also include extreme arrangements such as the zinc-blende and the sodium chloride structures.

The results from this test show that the zinc-blende structure has the lowest minimized energy, which is expected since this is structurally closely related to the stable low temperature structure of CuI (the $\gamma$ phase). A number of thermally populated low energy configurations are found where the coppers are distributed at tetrahedral sites *only* (i.e. the octahedral positions are all vacant). Overall, a significant fraction of about 20% of all arrangements make a considerable contribution at 750 K, contributing about 99% to the ensemble average. This indicates that a small set of randomly selected arrangements is sufficient for the present purpose. Still, it is important to emphasize that although a significant fraction of the minima is populated at 750 K, the majority of all configurations, including several in which the ions are distributed in the tetrahedral holes only, are *not* thermally accessible at high temperature. Furthermore, we

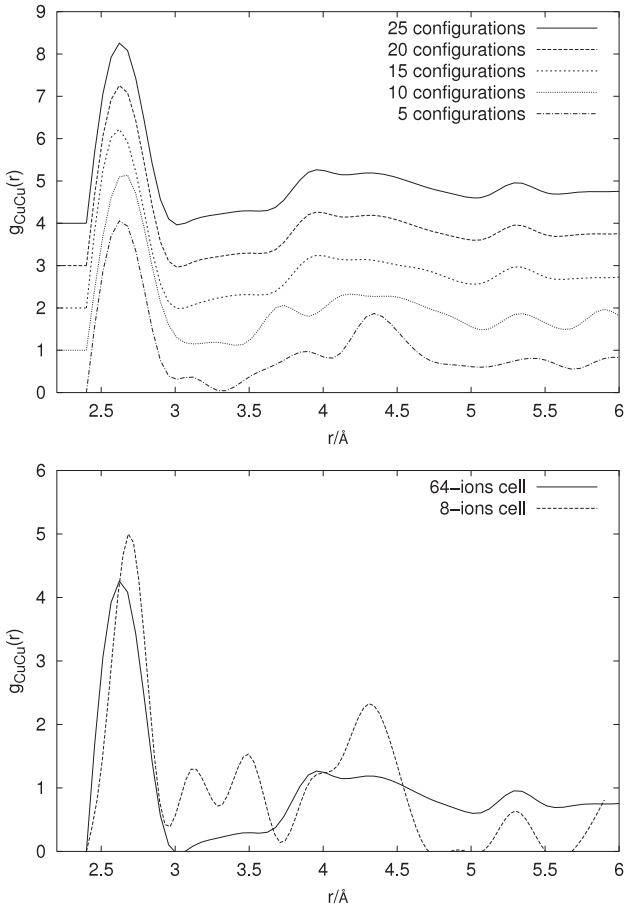


**Figure 3.** Convergence with number of randomly chosen configurations for the 64-atom simulation cell (top figure) and comparison between the results from eight-ion simulations and 64-ion simulations (bottom figure). In the top figure we plot the PDFs for 5, 10, 15, 20 and 25 randomly chosen configurations. Note the PDFs are shifted for clarity. All averagings are carried out at 750 K using equation (2.2).

found, in agreement with neutron diffraction [6], that *all* configurations where the octahedral site is also occupied are high in energy and unpopulated. The NaCl type structure was found to be highest in energy (0.42 eV/formula unit above the zinc-blende type structure in agreement with a previous DFT study [24]). Based on this preliminary test, we construct initial 64-atom configurations by distributing the Cu atoms among the tetrahedral 8c and 32f sites only, ignoring the 4b site.

In figure 3 we examine the convergence of the Cu–Cu PDF with number of randomly chosen configurations for the 64-atom cell carried out at 750 K using equation (2.2) (top figure), and in figure 3 (bottom figure) we compare the result from an eight-ion simulation (50 configurations were selected) with that of 25 randomly chosen configurations using a 64-ion simulation cell. As can be seen from the figure, the Cu–Cu PDF converges rapidly with the number of randomly chosen configurations and only a very few arrangements are required to give an overall qualitative description of the Cu–Cu PDF. 25 arrangements appear sufficient for the present purpose. Similar tests were carried out for the I–I and Cu–I partial PDFs and

the distribution of bond-angles. The comparison of the results from the two cells shows that a good qualitative agreement at short Cu–Cu distances ($r < 3$ Å) is found. However, the curves are markedly different at larger $r$ ($r > 3$ Å), which emphasizes that the results from the small eight-atom cell are influenced by some artificial features due to the constraints imposed by periodic boundary conditions. In the rest of the paper we therefore use the results from the 25 randomly chosen 64-atom arrangements to investigate in detail the structure of $\alpha$-CuI.

## 3. Results and discussion

### *3.1. The average structure*

In figure 4 we plot a projection of the fractional coordinates of the Cu atoms and the I atoms on an arbitrary face of the unit cell. The figure is constructed by applying the symmetry operations of the space group of the average structure ($Fm\bar{3}m$) on each of the populated optimized 64-atom configurations at 750 K.

The result is consistent with a previous crystallographic model of the structure where the Cu atoms were distributed at random at the 32f site (at $(x, x, x)$ etc with $x = 0.30$) [4, 5], but favours the recent model suggested by x-ray diffraction [9] where 80% of the coppers are randomly distributed at the 8c site and the remaining 20% are located at the 32f site (e.g. at $(x, x, x)$ etc with $x = 0.3360(17)$). In comparison, we find peaks in the atom density at the 8c site and the 32f site ($(x, x, x)$ etc with $x = 0.34$), with a higher occupancy of the former, in excellent agreement with the x-ray diffraction results of Yashima *et al* [9]. However, as can be clearly seen, the plot is very different from a model where the atoms are distributed at *distinct* sites since, in general, the iodines and the coppers are *both* displaced appreciably from these, in agreement with an RMC analysis of the ND data [25] and the recent x-ray powder diffraction study by Yashima *et al* [9].

It should be noted that the plot is generated in the static limit (without the inclusion of vibrations), which shows that the displacement away from the 8c site observed in x-ray powder diffraction experiments and ND-RMC is not *only* due to vibrations but *also* due to configurational disorder since the positions in figure 4 correspond to distinct minima on the potential energy surface.

### *3.2. Partial pair distribution functions*

The PDFs calculated using the CA method (equation (2.2)) at 750 K are plotted in figure 5 together with the integrated Cu–Cu and Cu–I curves (i.e. the average number of Cu and I respectively around a given Cu, which are extracted via equation (2.4)).

The following general comments regarding all partial PDFs should be noted. The partial PDFs calculated using the CA technique are more intense compared to experiment and results from MD simulations (in particular at short interatomic distances). However, the average coordination number is in agreement with experiment [6, 10]. This shows that the discrepancy between the PDFs in [6, 10] and ours is due to vibrations only. The PDFs are somewhat sensitive to the choice of the cutoff ($\Delta r$) in equation (2.2). A large cutoff (e.g. 0.3 Å) will create an artificial smearing of the correlation functions. However, if the cutoff is too small (e.g. 0.05 Å) the curves will be 'ragged' due to limitations in the amount of statistics available. Changing the cutoff from 0.1 to 0.25 Å has relatively little influence on all the main features (the relative intensities and the positions of the peaks). Similar tests were also carried out for the distribution of the coordination numbers and the bond-angles with the same conclusion.

The position of the first peak in the I–I PDF is located at approximately 4.3 Å in agreement with ND diffraction [6] and MD results [8, 11]. The correct position of this peak in the MD

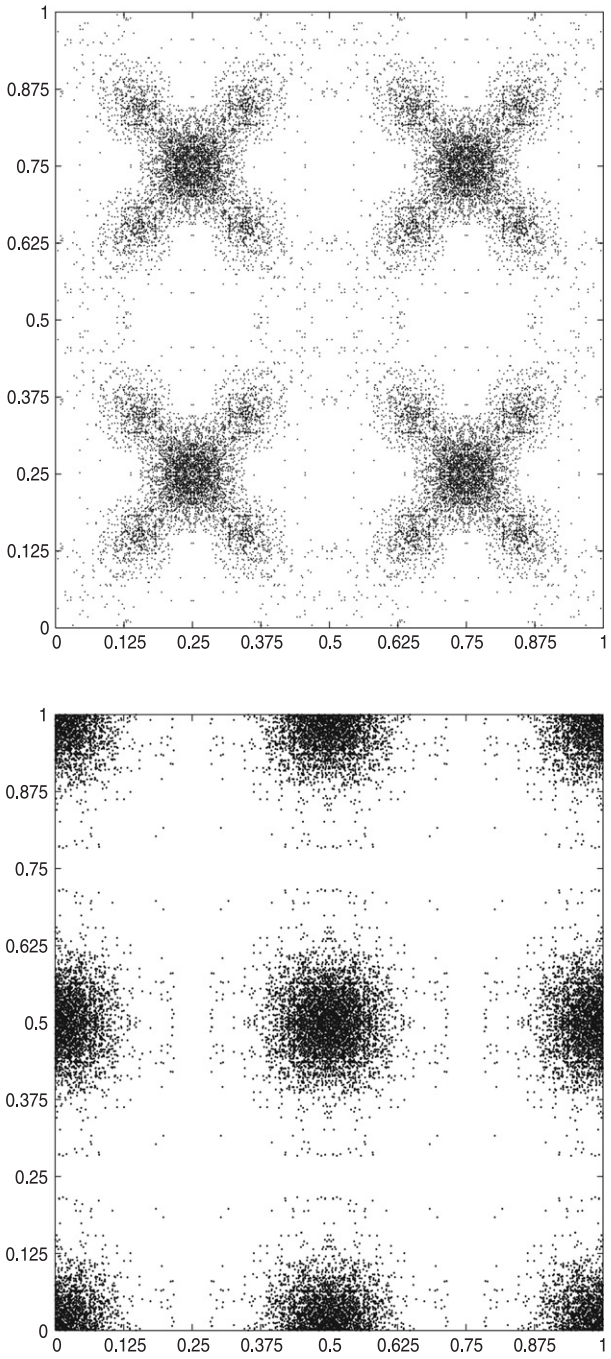


**Figure 4.** A projection of the fractional coordinates of Cu atoms (top figure) and I atoms (bottom figure) on an arbitrary face of the unit cell (e.g. the (100)-plane). The figure is generated by applying the symmetry operations of the average structure (space group $Fm\bar{3}m$) on each of the populated individual configurations at 750 K, and thus contains all symmetrically equivalent configurations of the thermally available optimized arrangements.

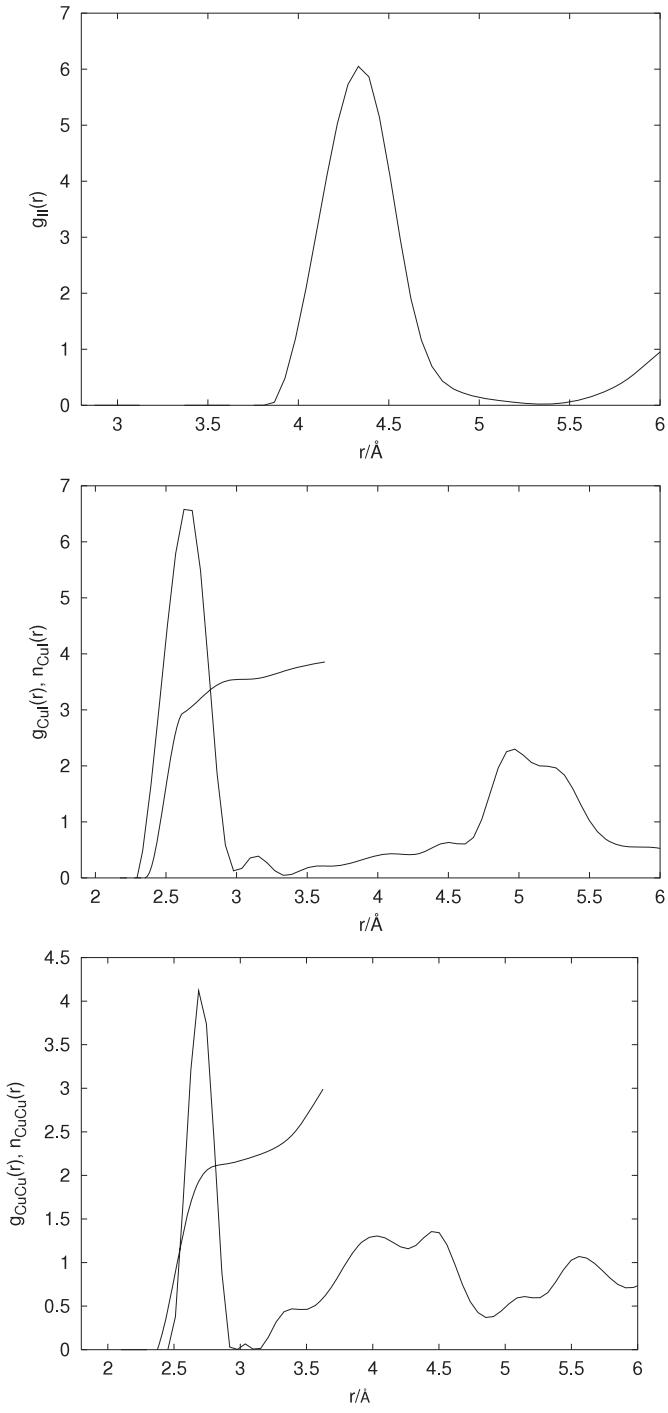


**Figure 5.** The partial I–I, Cu–I and Cu–Cu PDFs calculated using equation (2.2) at 750 K are shown as full lines, along with the integrated PDFs calculated using equation (2.4).

simulations reported in [8] and [11] is not surprising since the simulations are carried out in the $NVT$ ensemble using a cubic simulation box and the atom-density obtained from experiment. However, in contrast, since our calculations are carried out in the $NPT$ ensemble (we allow for

volume and cell-shape relaxations) the correct positions of this peak confirm that GGA is able to reproduce the experimental lattice parameters satisfactorily. Indeed, test calculations carried out using the local density approximation (LDA) show that the peaks in the I–I PDF are shifted to shorter distances compared to experiment. For example, the first peak was found at 3.9 Å using the LDA.

Comparing our I–I PDF to the ND-RMC result [6], we do not find evidence for a visible left-shoulder in the first peak in the I–I PDF, suggesting, in agreement with a recent structural reinvestigation of the ND total scattering value [10], that the marked left-shoulder is a spurious effect in the RMC analysis of the ND data due to low sensitivity at short interatomic distances of the total scattering. Although we ignore vibrations in this work, it is unlikely that the discrepancy between our results and that of ND-RMC is due to vibrations alone. Note that we also find a small peak at 6 Å consistent with the average face centred cubic sublattice of I atoms. This peak is smeared out due to vibrations in the *ab initio* MD simulations [11] and is also almost invisible in the ND-RMC result [6].

Turning to the Cu–I PDFs, we find a distinct first peak at approximately 2.6 Å and a less intense peak at roughly 5 Å. Although the positioning and relative intensities of these are in good agreement with all ND-RMC [6], EXAFS [10] and *ab initio* MD simulations [11], a detailed comparison reveals notable differences. Whereas the first peak in the ND-RMC has a visible left-shoulder with Cu–I bond-lengths as short as approximately 2.1 Å, the shape of the Cu–I PDF reported in this work is in better agreement with the EXAFS and *ab initio* MD results (i.e. without the distinct left-shoulder).

Turning to the Cu–Cu PDF we find a prominent peak at around 2.7 Å, a broader, less intense peak at roughly 4.3 Å and a small peak at around 5.4 Å, in agreement with the ND-RMC result [6]. However, the shape of the first peak in the Cu–Cu PDF calculated using CA is in better agreement with that of EXAFS, suggesting that the width of the first peak at around 2.7 Å is possibly exaggerated in the ND-RMC [6] and in the *ab initio* molecular dynamics [11], although vibrations must be included to draw firm conclusions. The failure of pair potentials to describe short range Cu–Cu interactions has been discussed previously (see e.g. [6]) and it has been suggested that the incorporation of three-body terms in the short range potential is crucial to describe this feature. The main discrepancy between results presented in this work and results from *ab initio* MD simulations reported in [11] is probably due to the lack of dynamics in the present study. However, the discrepancies between the PDFs in this work and the *ab initio* MD simulation in [11] may also be attributable to the different approaches taken. First, a rather coarse plane-wave energy cutoff for the electronic wavefunction (116 eV) was used in [11] which may give a poor description of the electronic structure and the PDFs. Test calculations carried out by systematically changing the energy cutoff indicate the presence of unphysical short Cu–Cu distances when the cutoff energy is less than approximately 150 eV. In addition, since the MD simulation in [11] is carried out for a few picoseconds only, the trajectory is visiting only a small (local) region on the Born–Oppenheimer surface, and may be hampered by insufficient sampling of the configurational space. By contrast, in this work we map the configurational space by selecting initial arrangements at random (we map very *different* regions of the configurational space simultaneously). In addition, we examine systematically the convergence of the PDFs with number of configurations. We have therefore shown that the CA method is not hampered by an insufficient sampling of the configurational space for $\alpha$-CuI. Although the PDFs were found to converge rapidly with number of configurations, we find in general that the PDFs of the individual optimized configurations are markedly different. With this in mind, it is also worth mentioning that there are cases [26] where MD simulations must be carried out over several nanoseconds to map with sufficient accuracy the configurational space of fast-ion conductors (in spite of the low diffusion barrier) which is unfeasible with *ab initio* MD.

Interestingly, as commented previously, the peak in the Cu–Cu PDF is at 2.7 Å which is at a significantly shorter distance compared to the shortest 8c–8c separation of the average structure and closer to an 8c–32f separation. However, the association of peak maxima with a particular separation between two distinct positions of an average structure is questionable, since the iodines are *also* displaced appreciably from their average positions.

### *3.3. Distribution of coordination numbers*

Comparison with experiment and *ab initio* MD in the previous section shows that the PDFs obtained with the CA method (excluding vibrations) in conjunction with GGA are in good agreement with experiment and *ab initio* DFT, and the CA method should thus provide a powerful and trustworthy tool to analyse in more detail the local structure of superionic CuI.

In figure 6 we plot the distribution of the coordination numbers of the coppers and iodines using equation (2.4) at 750 K. As can be seen from figure 6 the iodines show a range of coordination numbers. We find that about one third of the iodines are three-fold coordinated whereas roughly 50% are four-fold coordinated. An appreciable fraction are two-and five-fold coordinated. Less than 1% were six-fold coordinated and iodines with coordination lower than two were not found among the thermally populated arrangements.

Since the calculations of the coordination number involve only distances shorter than $r < 3.1$ Å ($r_{\max} = 3.1$ Å in equation (2.4)), it is important to analyse the sensitivity in the distribution in coordination numbers to the cutoff distance $r_{\max}$. Increasing the cutoff distance in equation (2.4) to $r_{\max} = 3.7$ we find that the relative distribution of the coordination numbers remains unchanged, but, as expected, the coordination numbers of a fraction of all iodines increase. The distribution of coordination numbers of coppers around the iodines is therefore not an artefact due to the cutoff chosen in equation (2.4), emphasizing that the iodines indeed show a variety of coordination numbers.

Investigating the local coordination around the coppers, we find that one third of the coppers are surrounded by three iodines and that two third are surrounded by four iodines. Although consistent with the model of average structure [9], where the majority of the coppers are near the four-coordinated 8c site and a large fraction is near the three-coordinated 32f site, we find in fact that many four-fold coppers are located near the 32f site and similarly that many three-fold coppers are near the 8c site. This is due to the highly flexible I-sublattice and emphasizes that the local structure may be very different from that of an average model.

The local coordinations of coppers around a given copper are also shown in figure 6. We find that the coppers can be bounded to as many as five Cu atoms although lower coordination numbers are more common. More specifically, we find that about 30% of all coppers are surrounded by two coppers in the first coordination shell whereas about 25% and 20% are surrounded by three and four coppers respectively. About 2% of the Cu atoms had as many as five coppers in their first coordination shell. Note that a significant fraction (about 20%) have just one Cu atom in their first coordination shell and about 4% have none.

### *3.4. Bond-angle distribution functions*

Having analysed the distribution of the coordination numbers, we now carry out a further analysis of the local structure by investigating the BAD. Although popular for analysing the local structure of amorphous systems, higher order correlation functions have, to our knowledge, not been investigated for superionic CuI. A few studies of BADs for superionic conductors have been reported; for example an MD study of superionic $Li_2O$ [27] using pair potentials and a recent Car–Parrinello MD study of the archetypal type-I superionic conductor $\alpha$-AgI [28].

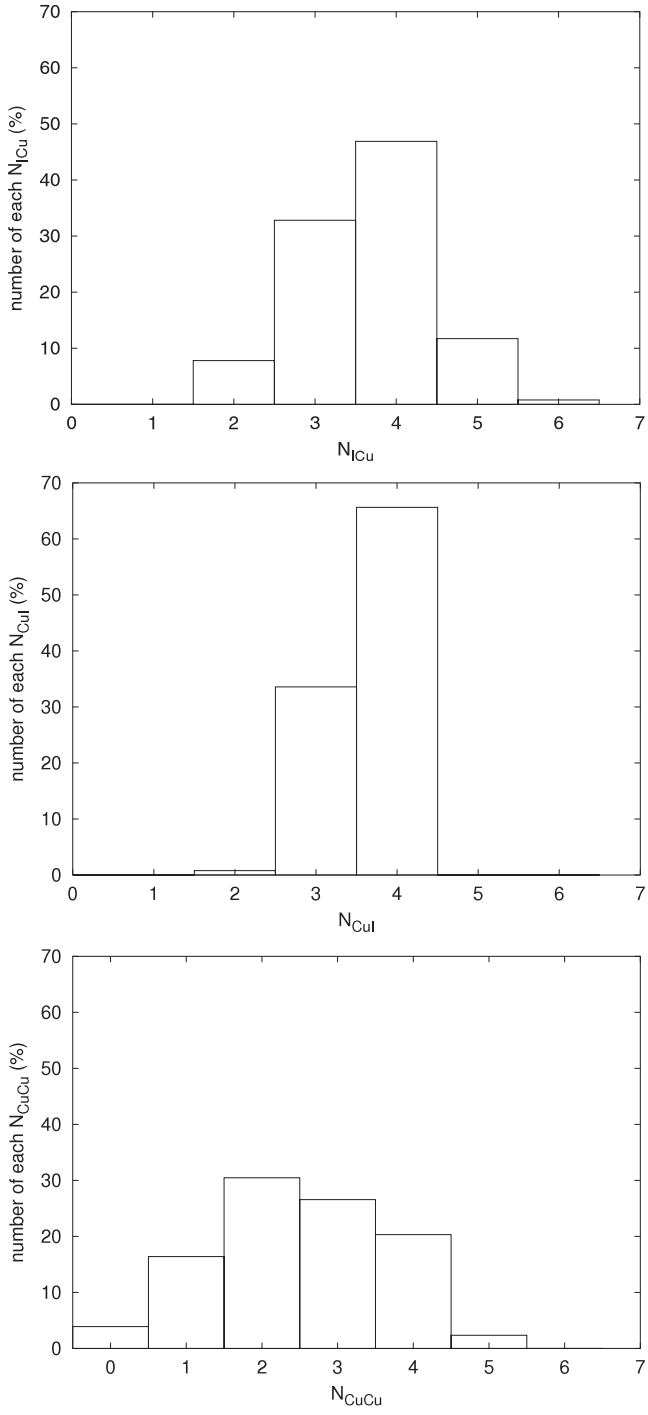


**Figure 6.** Distribution of coordination numbers calculated using equation (2.4) at 750 K. Top figure is the distribution of the coordination numbers of the coppers around the iodines, middle figure is the distribution of the CN of the iodines around the copper and bottom figure shows the distribution of the CN of the coppers around the coppers.

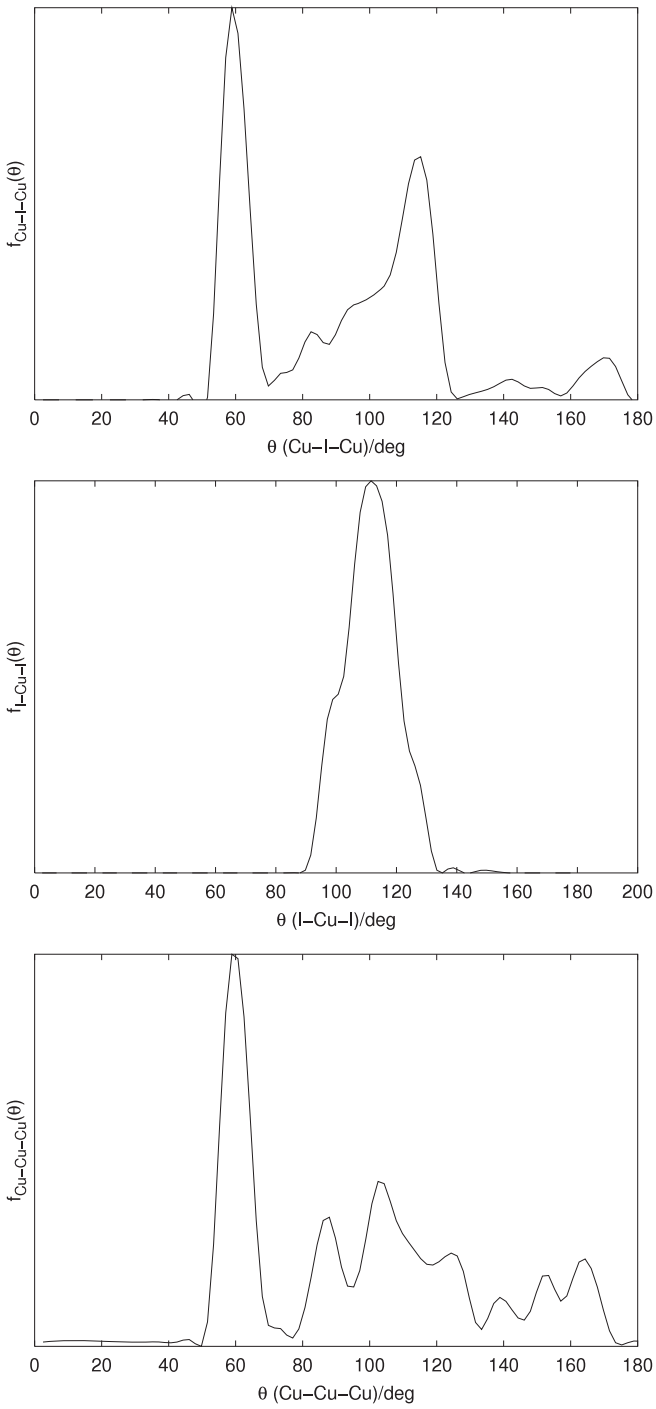


**Figure 7.** Cu–I–Cu (top figure), I–Cu–I (middle figure) and Cu–Cu–Cu (bottom figure) BADs calculated using equation (2.6) at 750 K.

The Cu–I–Cu BAD functions shown in figure 7 are smooth and show that a range of Cu–I–Cu bond-angles is found. The Cu–I–Cu BAD possesses one sharp and fairly symmetrical peak at approximately 60° and one broader peak at around 115° which is skewed to lower angles.

The Cu–I–Cu BAD is similar to the Ag–I–Ag BAD observed for the superionic AgI (obtained from an MD simulation [28]) where preferences for angles close to 65° and 110° were found.

Turning to the I–Cu–I BAD (see figure 7), a single smooth and prominent peak at around 110° is found, which is in agreement with a model of the average structure [9] due to the high occupancy of the tetrahedral 8c site (see figure 4 and [9]). However, interestingly, a further detailed investigation of the I–Cu–I BAD shows that the three- and four-fold coordinated coppers possess distinct peaks at different angles (i.e. at approximately 120° and 105°) which are not consistent with those expected from a model of the average structure. It is also worth commenting that although we do not plot the Cu–Cu–I BAD function, the locations of the peak maxima of the I–Cu–I BAD are not influenced by the penetration of coppers in the first coordination shell.

The Cu–Cu–Cu BAD (figure 7) is complex and emphasizes that the Cu–Cu–Cu angle is highly flexible. However, a clear preference for particular angles is obvious as the Cu–Cu–Cu BAD possesses a distinct peak at 60° with a marked right-shoulder. This is in contrast to a random distribution model based on the x-ray diffraction result [9] and that of figure 4 which predicts intense peaks around 90°.

### *3.5. Local structural snapshots*

The highly flexible bonds are of key importance in order to understand the exceptional transport properties of $\alpha$-CuI. This flexibility allows the I atoms to easily respond to changes in the local environment as the coppers diffuse, and a myriad of different diffusion trajectories is expected due to the large variation in the local motifs. This observation is consistent with the present model of the average structure, in that both the iodines and coppers are spread out [12]. A few examples emphasizing the variety of local environments around the iodines and the coppers are shown in figures 8 and 9.

Despite the inherent flexibility in the PDFs and BADs, we stress that the coppers are strongly correlated in their positions at short range; a position taken by a given copper is highly influenced by the positions of neighbouring coppers. This correlations manifests itself in distinct peaks in the PDFs and BADs which is different from expectations based on models of the average structure. The correlation is mainly short-ranged which is also evident from the width of the diffuse scattering from ND experiments [6]. Although the PDFs are very similar to that of liquid CuI [12], $\alpha$-CuI is *not* topological disordered since the iodines have the topology of a regular fcc lattice. The nature of the short range correlation and the topological packing constraints of the iodines have implications for local order beyond the first coordination shell. This is evident from a second peak in the Cu–Cu PDF which is almost absent in liquid CuI [12]. To visualize the local structure in $\alpha$-CuI also beyond the first coordination shell we plot in figure 10 a few examples of thermally available optimized arrangements representing realistic structural snapshots of the superionic phase. The difference between the average structure (figure 4) and the local structure (figure 10) is striking! As can be seen from the figures, the *instantaneous* structures show patterns of ‘holes’ and ‘channels’.

## 4. Concluding remarks

A detailed analysis of the average and local structure of $\alpha$-CuI has been carried out using configurational (Boltzmann) averaging in conjunction with DFT. The CA method presented in this work involves mapping the configurational space by optimizing a number of randomly chosen configurations followed by an appropriate Boltzmann average over the minimized potential energies. The CA method is particular advantageous in calculating properties

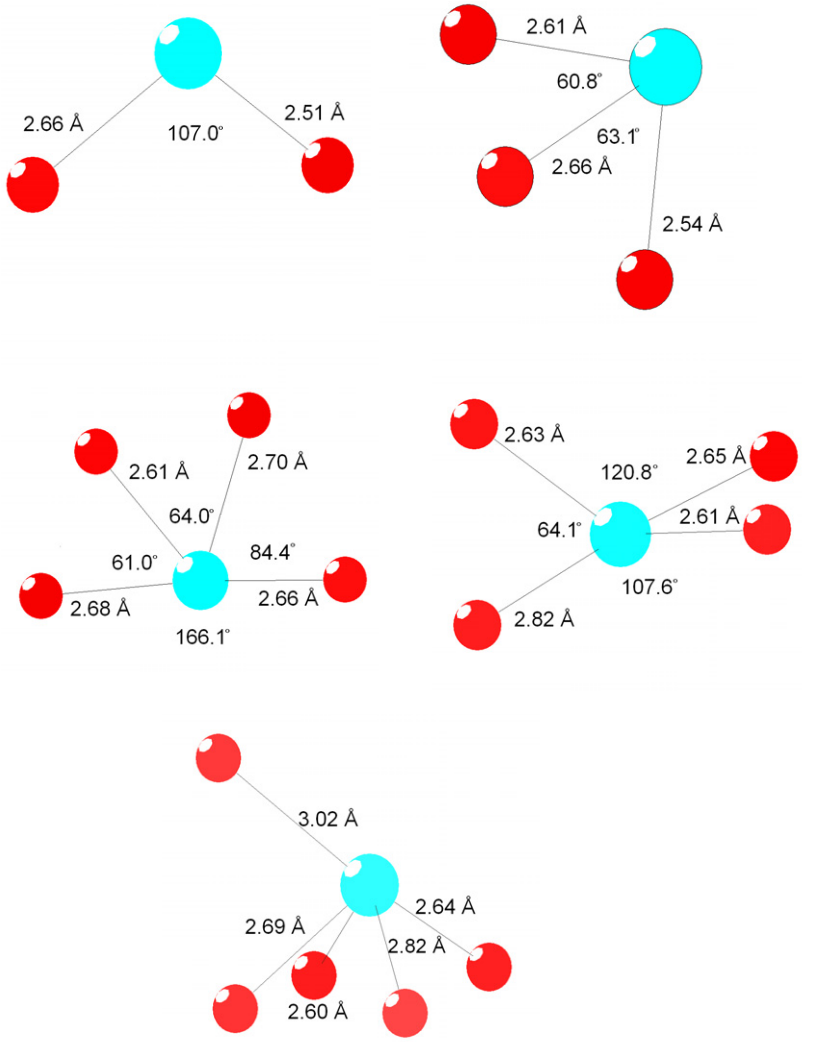


**Figure 8.** Examples of local entities with iodine as the central atom.

of disordered materials compared to conventional molecular dynamics in that it is not hampered by the presence of energy barriers and thus is ideally suited for studying long time dynamics. In addition, the CA method also allows a straightforward and unambiguous analysis of the structure since vibrational and configurational degrees of freedom can be treated separately.

We have carried out an analysis the convergence of the atom correlation functions (the PDFs) with number of configurations and discussed briefly cell-size effects. The PDFs converge rapidly with number of randomly chosen configurations and good agreement between the results from eight-atom and 64-atom simulations was obtained at short interatomic distances ($r < 3.0$ Å) but the PDFs obtained from the eight-atom cell are clearly hampered by the presence of some artificial features at $r > 3.0$ Å due to the restraints imposed by periodic boundary conditions. Our results support results from neutron diffraction [4, 5] and a recent x-

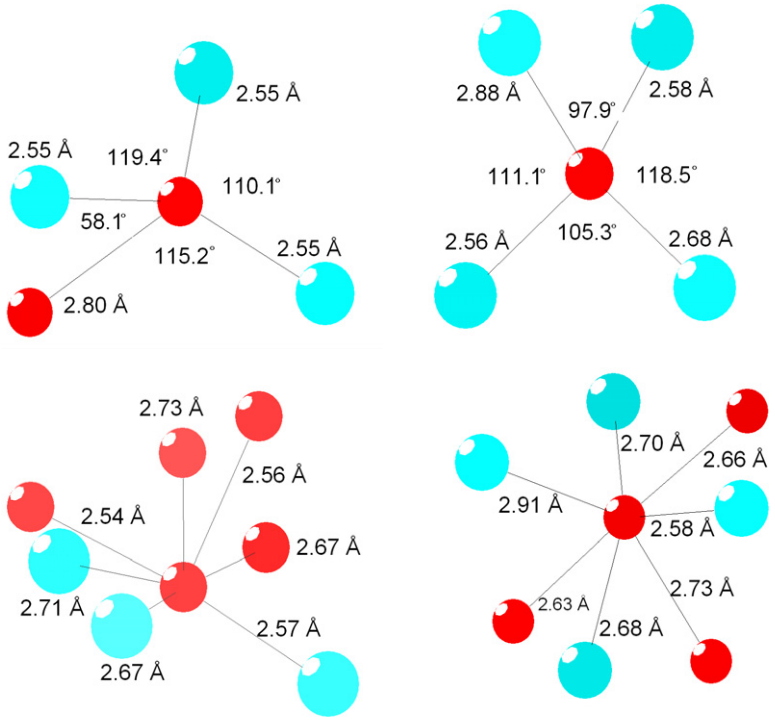


**Figure 9.** Examples of local entities with copper as the central atom.

ray diffraction study [9] in that atoms are located essentially in the tetrahedral cavities (i.e. the octahedral positions are all vacant) and spread out. The scattered atom-density observed in the present study is due to configurational disorder solely, since vibrations have been ignored.

We find that the partial PDFs calculated using the CA method in conjunction with the GGA are in good agreement with experimental ND-RMC and EXAFS results, although our peaks are too intense since we ignored vibrations. In particular, we find a single intense peak at 2.7 Å in the Cu–Cu PDF, in agreement with experiment and *ab initio* molecular dynamics simulation, showing that the coppers are strongly correlated at short distances. We also find a broad peak at roughly 4.3 Å in the Cu–Cu PDF, which arises essentially due to the topological packing constraints of the I sublattice. Furthermore, we do not find evidence for the presence of visible left-shoulders in the partial PDFs, suggesting, in agreement with recent structural reinvestigation of the ND total scattering value [10], that the marked left-shoulder in, for example, the I–I PDF is a spurious effect in the RMC analysis of the ND data.

A further detailed analysis of the local structure was carried out by investigating distributions of coordination numbers as well as distributions of Cu–I–Cu, I–Cu–I and Cu–Cu–Cu bond-angles. We find that the iodines take coordination numbers ranging from between two and five whereas the coppers allow the penetration of as many as five coppers within its first coordination shell. The Cu–I–Cu, I–Cu–I and Cu–Cu–Cu BADs are all smooth and broad. However, a marked preference for particular angles is found in all Cu–I–Cu, I–Cu–I and Cu–Cu–Cu BADs which are markedly different from those expected from a model based on the average structure.

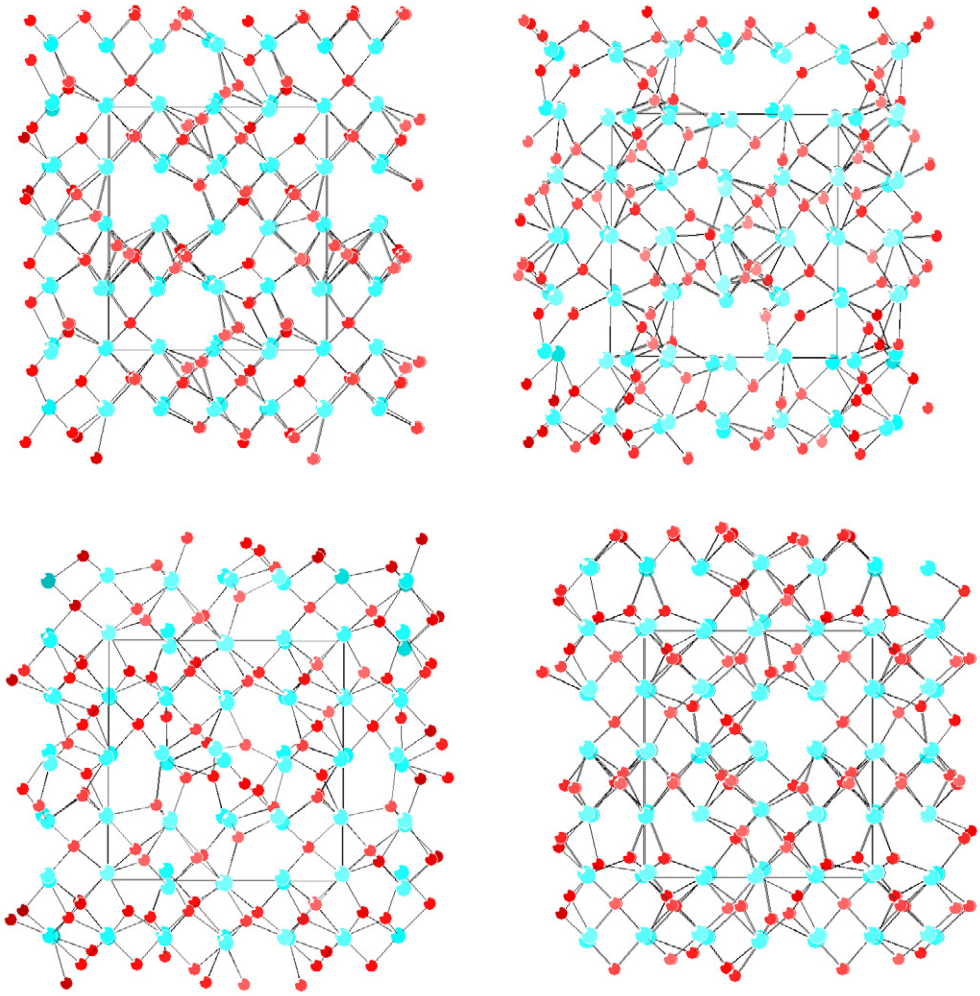

**Figure 10.** Examples of four optimized and thermally accessible (i.e. low energy) configurations. The unit-cells are shown for clarity. The large spheres represent the iodines whereas the smaller spheres are the coppers.

Together, the partial PDFs, the distribution of coordination numbers and the partial BADs allow a detailed analysis of the *local structure*. The large range of bond-lengths and bond-angles and the existence of a variety of coordination numbers is expected to be of key importance in order to understand the exceptional values of ion conductivity in $\alpha$-CuI: the inherent chemical and structural flexibility allows the I atoms to easily respond to changes in the local environment as the coppers diffuse and a myriad of different diffusion pathways is expected due to the large variation in the local structure.

## Acknowledgments

This work was funded by Norges Forskningsråd. Computational facilities were made available through a grant of computing time for the Programme of Supercomputing, Norway.

## References


[1] Krug J and Sieg L 1952 *Z. Naturf.* a **7** 369
[2] Boyce J B, Hayes T M and Mikkelsen J C Jr 1981 *Phys. Rev.* B **23** 2876
[3] Ihata K and Okazaki H 1997 *J. Phys.: Condens. Matter* **9** 1477
[4] Bűhrer W and Hălg W 1977 *Electrochim. Acta* **22** 701
[5] Keen D A and Hull S 1995 *J. Phys.: Condens. Matter* **7** 5793
[6] Chahid A and McGreevy R L 1998 *J. Phys.: Condens. Matter* **10** 2597
[7] Hull S 2004 *Rep. Prog. Phys.* **67** 1233
[8] Zheng-Johansson J X M, Ebbsjö I and McGreevy R L 1995 *Solid State Ion.* **82** 115
[9] Yashima M, Zu Q, Yoshiasa A and Wada S 2006 *J. Mater. Chem.* **16** 4393
[10] Trapananti A, Cicco A D and Minicucci M 2002 *Phys. Rev.* B **66** 014202
[11] Shimojo F and Aniya M 2003 *J. Phys. Soc. Japan* **72** 2702
[12] Wasada Y, Kang S, Sugiyama K, Kimura M and Saito M 2000 *J. Phys.: Condens. Matter* **12** A195
[13] Allan N L, Barrera G D, Fracchia R M, Lavrentiev M Y, Taylor M B, Todorov I T and Purton J A 2001 *Phys. Rev.* B **63** 094203
[14] Bakken E, Allan N L, Barron T H K, Mohn C E, Todorov I T and Stølen S 2003 *Phys. Chem. Chem. Phys.* **5** 2237
[15] Mohn C E, Allan N L, Freeman C L, Ravindran P and Stølen S 2005 *J. Solid State Chem.* **178** 346
[16] Sarnthein J, Schwarz K and Blöchl P E 1996 *Phys. Rev.* B **53** 9084
[17] Mohn C E 2005 Computational studies of the potential energy hypersurface of disordered systems—linking structure, energetics and dynamics *PhD Thesis* University of Oslo
[18] Perdew J P and Wang W 1992 *Phys. Rev.* B **45** 13244
[19] Kresse G and Hafner J 1993 *Phys. Rev.* B **47** 558
[20] Kresse G, Joubert J and Hafner J 1999 *Phys. Rev.* B **59** 1758
[21] Mohn C E, Allan N L, Freeman C L, Ravindran P and Stølen S 2004 *Phys. Chem. Chem. Phys.* **6** 3052
[22] Mohn C E and Stølen S 2005 *J. Chem. Phys.* **123** 114104
[23] Cienfuegos C, Isoardi E P and Barrera G D 2005 *Phys. Rev.* B **71** 144202
[24] Söhnel T, Hermann H and Schwerdtfeger P 2005 *J. Phys. Chem.* B **109** 526
[25] Chahid A and McGreevy R L 1997 *Physica* B **234** 87
[26] Hamakawa S, Aniya M and Shimojo F 2005 *Solid State Ion.* **176** 2471
[27] Goel P, Choudhury N and Chaplot S L 2004 *Phys. Rev.* B **70** 174307
[28] Wood B C and Marzari N 2006 *Phys. Rev. Lett.* **97** 166401